Monthly Notices
of the
ROYAL ASTRONOMICAL SOCIETY

MNRAS **451,** 2145–2160 (2015) doi:10.1093/mnras/stv1021

Bibliographic review and new measurements of the infrared band strengths of pure molecules at 25 K: H_2O, CO_2, CO, CH_4, NH_3, CH_3OH, HCOOH and H_2CO

M. Bouilloud,* N. Fray,* Y. Bénilan,* H. Cottin, M.-C. Gazeau and A. Jolly

Laboratoire Interuniversitaire des Systèmes Atmosphériques (LISA), UMR CNRS 7583, Université Paris Est Créteil et Université Paris Diderot, Institut Pierre Simon Laplace, 61 Avenue du Général de Gaulle, F-94010 Créteil Cedex, France

Accepted 2015 May 6. Received 2015 May 5; in original form 2014 October 27

ABSTRACT

Infrared observations of the interstellar medium revealed the presence of several molecules in the solid phase such as H_2O, CO_2, CO, CH_4, NH_3, CH_3OH, H_2CO and HCOOH. Measurements of column densities and molecular abundances relative to water require the knowledge of infrared band strengths. We present a review of refractive indices at visible wavelengths, densities and infrared band strengths for all eight molecules. We also present new band strengths measured on icy films whose thicknesses have been determined using laser interference techniques. For CO_2, CO, CH_4 and NH_3, our measurements are in agreement with previous determinations taking into account an uncertainty of about 20 per cent. For H_2O ice films, the porosity and the density remain unreliable, leading to large uncertainties on the measured band strengths. Concerning amorphous CH_3OH, H_2CO and HCOOH, the densities and refractive indices are unknown leading to large uncertainties on the band strengths. However, we propose new values that are slightly different from previous determination. Our review and experimental work point out the most reliable band strengths for the eight studied molecules. For CH_4, CH_3OH, HCOOH and H_2CO, the band strengths used to calculate abundances in the ices of interstellar medium seem to be inaccurate, leading to some doubts on the determined values.

Key words: molecular data – methods: laboratory: molecular – methods: laboratory: solid state – ISM: abundances – infrared: ISM.

1 INTRODUCTION

Numerous simple molecules are present in the icy dust grain mantles in the different environments of the interstellar medium (ISM). The molecular composition of the condensed phase can be investigated using infrared spectroscopy. The access to the mid-infrared range, with infrared space telescopes such as *Infrared Space Observatory* (*ISO*) and *Spitzer*, allowed the detection and quantification of molecular components in icy grains. Around young stellar objects (YSOs), the presence of solid H_2O, CO, CO_2, CH_3OH, NH_3, CH_4, HCOOH and H_2CO has been revealed (Gibb et al. 2004; Dartois 2005; Boogert et al. 2008; Oberg et al. 2011). Positions and shapes of infrared bands are useful to constrain the nature of these ices (Pontoppidan et al. 2008). The column densities and the abundances of these molecules relative to water are retrieved using the infrared band strengths. The abundances relative to H_2O of CO_2 and CO are about 10 per cent and for CH_3OH, NH_3 and CH_4 only of a few per cent (Oberg et al. 2011). Boogert et al. (2008) have also estimated the abundance relative to H_2O around a low-luminosity YSO for solid HCOOH (1–5 per cent) and H_2CO (6 per cent). The determination of these abundances is essential to investigate the chemical evolution of ices during star formation.

The infrared band strength, which is generally noted A (cm molecule^{-1}), is the key value to retrieve column densities and molecular abundances relative to water. A-values are mostly studied for gas phase molecules and there is a lack of information for the solid phase. This is also true for the optical indices (n) and the densities (ρ) of the solid phases, which are necessary to calculate the column densities N (molecules cm^{-2}) and the band strengths. It has already been shown by Brunetto et al. (2008) that some band strengths in the literature are suspicious. Moreover, many approximations in the calculations, generally related to the values of the optical indices and densities, make the determination sometimes doubtful. For examples, d'Hendecourt & Allamandola (1986) and Hudgins et al. (1993) have assumed a density of 1 g cm^{-3} for all the studied ices.

The aim of this paper is to provide band strength values measured under the same conditions for eight molecules. First, we review the published values for pure ices concerning optical indices in the visible wavelength domain and densities. Then we present new

*E-mail: michaelle.bouilloud@lisa.u-pec.fr (MB); nicolas.fray@lisa.u-pec.fr (NF); yves.benilan@lisa.u-pec.fr (YB)

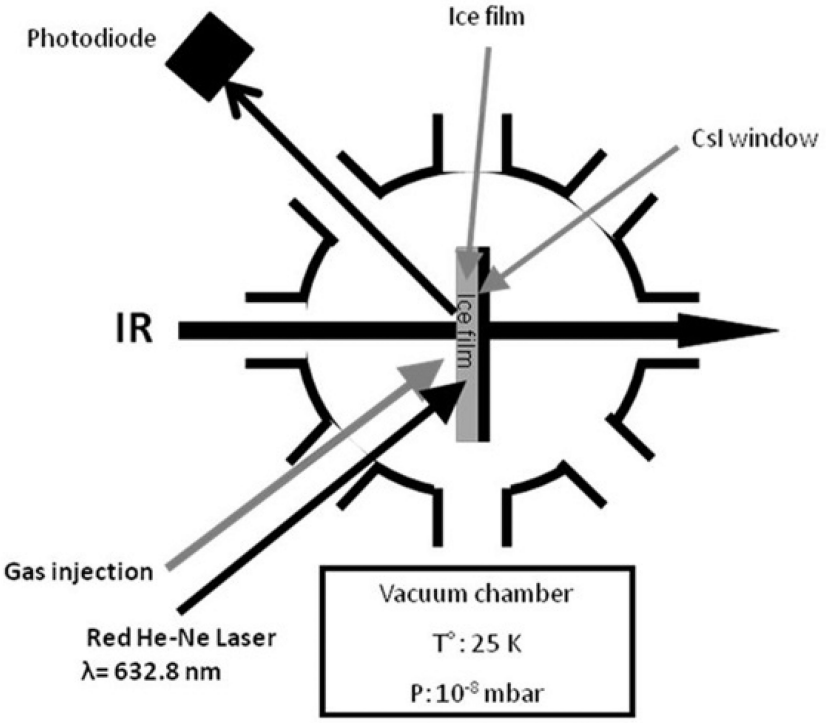

Figure 1. Experimental setup includes a high vacuum chamber connected to a gas injection line, a FTIR spectrometer, and a laser-photodiode system.

band strengths measured at low temperature (25 K) for molecules known to be present in the ISM in condensed phase.

2 EXPERIMENTAL SETUP AND PROCEDURE

Our experimental apparatus has already been described in Le Roy et al. (2012) and Briani et al. (2013). We use a high vacuum chamber connected to a gas injection line, a FTIR spectrometer to measure the infrared transmission of the ice film and a laser-photodiode system to quantify the thickness of the ice film (see Fig. 1).

2.1 The high vacuum chamber

The high vacuum chamber is maintained at about 10^{-8} mbar using a turbo pump (Varian turbo-V 301) backed up by a primary pump (Varian SH110). A 10 mm diameter CsI window is located at the centre of this chamber and is connected to a closed cycle helium cryostat via a resistive heater. A thermocouple (Au—Fe–Cr) and a platinum resistor are fixed between the resistive heater and the CsI windows. The temperature sensors and the resistive heater are connected to a temperature controller (Lakeshore 340) that regulates the temperature of the CsI window by means of a proportional-integral-derivative (PID) feedback algorithm. In this study, the window temperature is stabilized at 25 K.

The studied molecules are injected in gas phase and condensed on the CsI window at 25 K. The injection gas line is located at 10 cm from the CsI window and the angle between the gas injection line and the normal of the CsI window is 45° (see Fig. 1). A micrometric valve regulates the gas flow towards the vacuum chamber and the upstream pressure is measured with an absolute Baratron (MKS 627 B). We monitor the icy film deposition measuring simultaneously the thickness with a red He–Ne laser ($\lambda = 632.8$ nm) – photodiode system in reflection and the infrared transmission of the ice (see Fig. 1). The compounds used in this study are H_2O (liquid, triply distilled); CH_3OH (liquid, Sigma-Aldrich 99.9 per cent); CO (gas, Air Liquide 99.997 per cent); CO_2 (gas, Air Liquide 99.998 per cent); NH_3 (gas, Air Liquide 99.999 per cent); CH_4 (gas, Air Liquide 99.995 per cent); HCOOH (liquid, Merck, >99 per cent); H_2CO (Polyoxymethylene, Prolabo, 95 per cent). The polyoxymethylene commonly named POM is a solid formaldehyde polymer used to form gaseous formaldehyde by slow thermal decomposition.

2.2 The infrared spectrometer

The icy films are analyzed by transmission in the infrared using a Bruker Vertex 70 FTIR spectrometer coupled with a Mercury–Cadmium–Telluride (MCT) detector. This detector is located outside of the spectrometer and the high vacuum chamber. The optical path outside the high vacuum chamber is purged with a flow of dry air. At the entrance and exit of the vacuum chamber, the IR beam goes through two ZnSe windows. The CsI window, on which the ice film is prepared, is oriented at normal incidence with respect to the IR beam. Spectra were recorded in the mid-IR (600–5000 cm^{-1}) range with 1 cm^{-1} resolution. Each spectrum corresponds to an average of 256 scans. Note that the original software calculates absorbance with a decimal logarithm. In this study, all the absorbance spectra have been converted in optical depth spectra with a natural logarithm.

2.4 Band strengths and column densities of ice films

The purpose of this study is to provide accurate values of the band strengths for the main absorption bands of H_2O, CO_2, CO, CH_4, NH_3, CH_3OH, HCOOH and H_2CO in the mid-infrared range. The Beer–Lambert law can be written as:

$$I_t(\bar{\nu}) = I_0(\bar{\nu})e^{-\sigma(\bar{\nu})N} \quad (1)$$

where $I_0(\bar{\nu})$ and $I_t(\bar{\nu})$ are the incident and transmitted intensities for a given wavenumber $\bar{\nu}$ (cm^{-1}), N the column density of the ice film (molecules cm^{-2}) and $\sigma(\bar{\nu})$ the absorption cross-section (cm^2). Equation (1) can also be written as:

$$\sigma(\bar{\nu}) = \frac{1}{N} \ln\left(\frac{I_0(\bar{\nu})}{I_t(\bar{\nu})}\right) = \frac{1}{N}\tau(\bar{\nu}), \quad (2)$$

where $\tau(\bar{\nu})$ is the optical depth for a given wavenumber $\bar{\nu}$ (cm^{-1}). Finally, equation (2) is integrated for a given absorption band to get the infrared band strength A (cm molecule^{-1}):

$$A = \frac{1}{N}\int \tau(\bar{\nu})\, d\bar{\nu} = \int \sigma(\bar{\nu})\, d\bar{\nu}. \quad (3)$$

To determine the band strengths A in the laboratory, the column density N of the ice films is required. It is determined independently from the interference pattern measured in reflection with the He–Ne laser-photodiode system and recorded during the ice film deposition. Indeed:

$$N = \frac{t.\mathrm{p.Na}}{M} \quad (4)$$

where ρ is the density of the considered pure ice (in g cm^{-3}), M is the molecular mass (g mol^{-1}), Na is the Avogadro constant (molecule s mol^{-1}) and t is the ice thickness (cm).

The thickness t is obtained from a technique developed by Hollenberg & Dows (1961), which consists in counting the number of fringes in the interference pattern as a function of the deposition time. The number of fringes (k) can then be converted into a thickness t using the following equation:

$$t = k\frac{\lambda}{2n \times \sqrt{1 - \left(\frac{\sin(i)}{n}\right)^2}}, \quad (5)$$

where λ is the wavelength of the He–Ne laser ($\lambda = 632.8$ nm), n the refractive index of the studied ice at the laser wavelength and i the angle of incidence of the laser beam on the film surface ($i = 45°$ in this study). The observed interference pattern has been adjusted with an in-house code allowing the determination of the number of fringes (k) as a function of the deposition time (see Fig. 2).

Note that we need to know the refractive indices n in the visible wavelength domain and the densities ρ of the studied ices to determine the column densities. In the following section, we will present a bibliographic review for both parameters.

Fig. 2 presents an example of an interference pattern recorded during the deposition of a CH_4 film at 25 K as a function of time, as well as the corresponding thickness and column density obtained with a refractive index of 1.34 and a density of 0.45 g cm^{-3} (see the next section).

During the formation of the ice films, the interference pattern and the IR spectra are monitored simultaneously. This allows us to measure the evolution of the infrared absorbance and the corresponding column density of the film. The band strength can then be obtained from the slope of the integrated optical depth as a function of the column density [equation (3) and Fig. 3]. To retrieve the slope, a linear fit, constrained to pass through the origin, has been performed. The integration of all the absorption bands has been obtained with an in-house code after subtracting a baseline using a second-order polynomial. For each molecule, this procedure has been repeated four times with identical experimental conditions but different deposition rates, ranging from 10^{14} to 5×10^{15} molecules cm^{-2} s^{-1}, depending on the considered molecule.

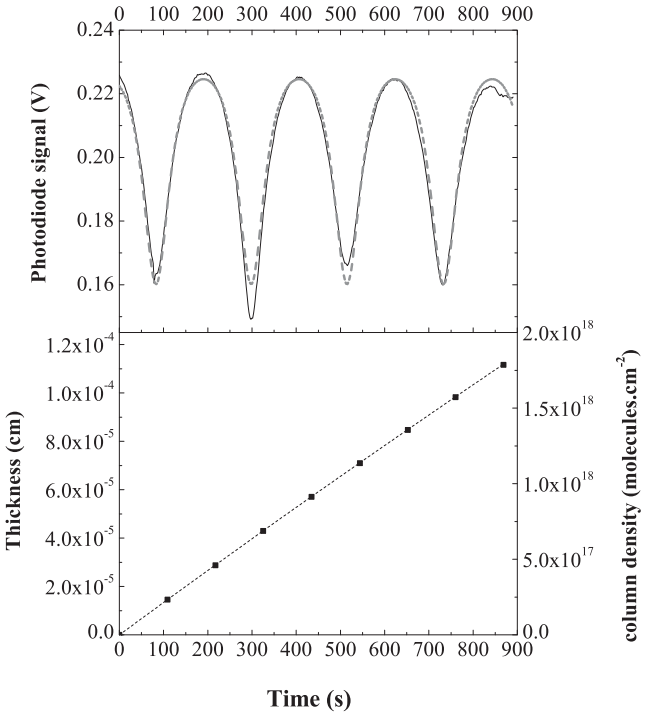

Figure 2. Interference pattern recorded as a function of time during the deposition of a CH_4 ice film. Top panel: observed (full line) and adjusted (dashed line) interference pattern. Bottom panel: thickness and column densities (black points) calculated using a refractive index of 1.34 and a density of 0.45 g cm^{-3}.

Note that the pressure in the vacuum chamber is about 10^{-8} mbar. Even if no intentional deposition is performed, we can observe without any injection some interference patterns with a period of about 10^5 s corresponding roughly to a background deposition of 10^{13} molecules cm^{-2} s^{-1}. When preparing icy films for the infrared measurements, we used higher deposition rates ranging from 10^{14} to 5×10^{15} molecules cm^{-2} s^{-1} and consider that the contribution of the background deposition can be neglected.

3 BIBLIOGRAPHIC REVIEW OF THE REFRACTIVE INDICES IN THE VISIBLE AND OF THE DENSITY OF PURE ICES OF H_2O, CO_2, CO, CH_4, NH_3, CH_3OH, H_2CO AND HCOOH

In this section, we present the refractive indices and the densities found in the literature for pure ices: H_2O, CO_2, CO, CH_4, NH_3, HCOOH, CH_3OH, H_2CO. The published values are presented in Table 1 and the preferred values that will be used to calculate the band strengths are summarized in Table 2. In general, the refractive indices are measured by a dual-angle laser system whereas densities are deduced from quartz micro-balance measurements (Wood & Roux 1982; Satorre et al. 2008).

3.1 H_2O (water)

Numerous studies dealing with the physical properties of amorphous solid water have already been published. At least three different amorphous phases of water ice exist depending on the preparation routes and the sample history. We can distinguish low density amorphous (LDA), high density amorphous (HDA) and very high density amorphous water ice (VHDA; Loerting et al.

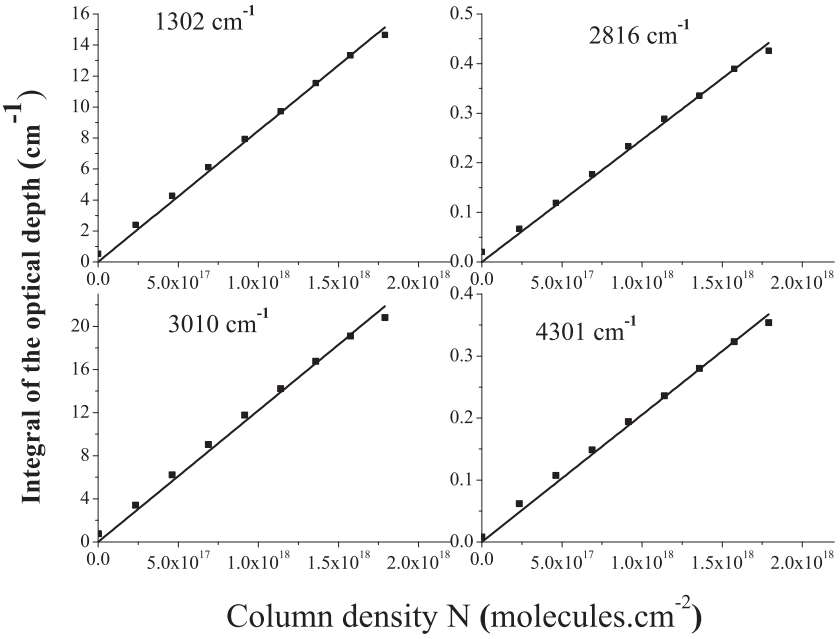

Figure 3. Integrated optical depth values of four bands of CH_4 as a function of the column density. The squares represent the experimental data, and the straight line is a linear fit.

Table 1. Published values of the refractive indices and densities of pure ices at low temperatures.

Molecule	T° (K)	Refractive index at 632.8 nm	Density (g cm^{-3})	Reference
H_2O	82		0.81	Seiber et al. 1970
	30–135		0.94	Ghormley & Hochanad 1971
	10		1.1	Narten 1976
	77		0.94	Narten 1976
	20–50–80	1.32		Wood & Roux 1982
	20–140	1.316		Warren 1986
	82	1.26	0.80 ± 0.01	Berland et al. 1995
	20	1.19	0.6	Brown et al. 1996
	90	1.27	0.8	Brown et al. 1996
	130	1.31	0.93	Brown et al. 1996
	20–140	1.29 ± 0.01	0.82 ± 0.01	Westley, Baratta & Baragiola 1998
	22	1.285 at $< 40^{\circ}$	0.94 at $< 40^{\circ}$	Dohnalek et al. 2003[a]
	22	1.27 at 45°	0.87 at 45°	Dohnalek et al. 2003[a]
	22	1.05 at 86°	0.16 at 86°	Dohnalek et al. 2003[a]
	80	1.29 ± 0.01		Romanescu et al. 2010
CO_2	25	1.3	1.15	Schulze & Abe 1980
	20	1.28	1.08	Wood & Roux 1982
	25	1.25	1.1	Satorre et al. 2008
CO	20	1.22 ± 0.02		Pipes et al. 1978
	20	1.27	0.80	Roux et al. 1980
CH_4	20	1.38 ± 0.02		Pipes et al. 1978
	20	1.35	0.426	Roux et al. 1980
	10–35	1.30 ± 0.02	0.47	Satorre et al. 2008
	16	1.329	0.403	Brunetto et al. 2008
NH_3	20	1.42 ± 0.02		Pipes et al. 1978
	20	1.37	0.76	Wood & Roux 1982
	25	1.44 ± 0.1		Dawes et al. 2007
	20	1.40 ± 0.03	0.72 ± 0.05	Satorre et al. 2013
	15	1.36 ± 0.01		Zanchet et al. 2013
	30	1.38 ± 0.01		

[a]The indicated angle is the deposition angle, i.e. the angle between the normal incidence of the windows and the gas injection line.

Table 2. List of the low temperature refractive indices n and densities ρ used to calculate the band strengths in this work.

Molecule	n	ρ (g cm^{-3})
H_2O	1.27 ± 0.02	0.87 ± 0.03
CO_2	1.27 ± 0.02	1.11 ± 0.03
CO	1.25 ± 0.03	0.80 ± 0.01
CH_4	1.34 ± 0.04	0.45 ± 0.03
NH_3	1.41 ± 0.04	0.74 ± 0.02
CH_3OH	1.33 ± 0.04	1.01 ± 0.03
HCOOH	1.37 ± 0.04	1.22 ± 0.03
H_2CO	1.33 ± 0.04	0.81 ± 0.03

2011). The value of 0.94 g cm^{-3} for the intrinsic density (not including micro-pores) measured by Ghormley & Hochanad (1971) and Narten (1976) on LDA ice seems to be accepted. The values lower than 0.94 g cm^{-3}, which are presented in Table 1, correspond to the bulk densities which include pores. As we will see in the next section, we observed in our experiments the dangling mode of water ice, which proves that we have formed a porous water ice film. Thus, we consider a density value lower than 0.94 g cm^{-3} to calculate column densities. Our experimental conditions are similar to the work of Dohnalek et al. (2003) who found a density of 0.87 g cm^{-3}. Nevertheless, we have to keep in mind that amorphous water ice could have even lower densities at low temperature (Seiber et al. 1970; Brown et al. 1996; Dohnalek et al. 2003).

Concerning the refractive index, we will also use the value found by Dohnalek et al. (2003) for a deposition angle of 45°, i.e. $n = 1.27$, which is in close agreement with other measurements (see Table 1).

3.2 CO_2 (carbon dioxide)

The values of refractive index of CO_2 ice given in Table 1 complement those already reviewed by Warren (1986). For CO_2, numerous authors (Schulze & Abe 1980; Wood & Roux 1982; Satorre et al. 2008) have observed a significant increase of the refractive index and density with the deposition temperature. For example Satorre et al. (2008) measured optical indices between 1.21 and 1.36 and densities between 1 and 1.5 g cm^{-3} for icy CO_2 from 10 to 80 K. Those observations show that the structure of the CO_2 ice film depends on the temperature. The density increase with increasing temperature could be due to the formation of porous and amorphous ice films at low temperature (Escribano et al. 2013). The values of the refractive index and density measured by Schulze & Abe (1980), Wood & Roux (1982) and Satorre et al. (2008) at 20–25 K are in good agreement. Thus we choose an average of those three values, i.e. $n(CO_2) = 1.27 \pm 0.02$ and $\rho(CO_2) = 1.11 \pm 0.03$ g cm^{-3} (see Tables 1 and 2).

3.3 CO (carbon monoxide)

To our knowledge, only two values of the refractive index of CO ice are available in the literature. Those have been obtained by gas condensation at 20 K in the visible domain (Pipes et al. 1978; Roux et al. 1980; see Table 1). In this study, we use an average, i.e. $n(CO) = 1.25 \pm 0.03$. Concerning the density of CO ice prepared by gas condensation at low temperature, we found only one value (Roux et al. 1980; see Table 1). Thus, we choose to use $\rho(CO) = 0.80 \pm 0.01$ g cm^{-3}.

3.4 CH_4 (methane)

For CH_4, several values of the refractive index and density have been published (see Table 1). Four values of refractive index (Pipes et al. 1978; Roux et al. 1980; Brunetto et al. 2008; Satorre et al. 2008) have been measured from gas condensation at temperatures between 10 and 35 K. These values spread from 1.30 to 1.38. We have chosen to use an average, i.e. $n(CH_4) = 1.34 \pm 0.04$. Concerning the density of CH_4 ice, we found two direct measurements using the quartz micro-balance technique (Roux et al. 1980; Satorre et al. 2008). The density values are 0.426 and 0.47 g cm^{-3} (see Table 1). As for the refractive index, we have chosen to use an average, i.e. $\rho(CH_4) = 0.45 \pm 0.03$ g cm^{-3}. Note that Satorre et al. (2008) do not observe any variations of the refractive index (at 632.8 nm) and of the density for temperature deposition between 10 and 35 K.

3.5 NH_3 (ammonia)

The densities and refractive indices of NH_3 available in the literature have been recently reviewed by Satorre et al. (2013). Table 1 also includes new measurements by Zanchet et al. (2013). Satorre et al. (2013) performed numerous new measurements between 13 and 100 K. The properties of NH_3 ices do not vary significantly for temperature higher than 60 K. But for lower temperatures, the refractive index and the density increase with temperature. For temperatures lower than 30 K, we found five measurements of the refractive index (see Table 1) which are in good agreement. Thus, we used an average value, i.e. $n(NH_3) = 1.41 \pm 0.04$. Concerning the density, only Satorre et al. (2013) and Wood & Roux (1982) performed measurements at temperatures lower than 60 K for NH_3 ice. As their values are in agreement, we use the average, i.e. $\rho(NH_3) = 0.74 \pm 0.02$ g cm^{-3}.

3.6 CH_3OH, HCOOH and H_2CO (methanol, formic acid and formaldehyde)

For CH_3OH, HCOOH and H_2CO, no measurements of the refractive indices and densities for pure solid molecules at low temperatures have been published. Hudgins et al. (1993) used the refractive indices of the liquid phase for CH_3OH. To compare with our measured band strengths, we also use the values of the liquid phase (Weast & Astle 1985), i.e. 1.33 and 1.37 for CH_3OH and HCOOH, respectively.

Concerning H_2CO, no value of the refractive index has been found in the literature. We arbitrarily considered a refractive index of 1.33 which corresponds to an average of the values for the other molecules.

Regarding the CH_3OH density, we found no measurements for the amorphous phase at low temperature. Therefore, we take the value of Mate et al. (2009) i.e. $\rho(CH_3OH) = 1.01$ g cm^{-3} which is derived from the diffraction measurements of Torrie et al. (2002) on the crystalline α-phase. Concerning HCOOH and H_2CO, we found no measurement of the density for the solid phase. The density employed in this work for both molecules are those of the liquid. Those values are 1.22 and 0.81 g cm^{-3} for HCOOH and H_2CO, respectively (Weast & Astle 1985).

4 RESULTS AND DISCUSSION

Tables 3–10 present the band strengths found in the literature compared to our own results. Discrepancies can be due to different density values. For example d'Hendecourt & Allamandola (1986)

Table 3. Assignments and band strengths of H_2O ice.

Label	Mode	Position cm^{-1}	Wavelength μm	T K	n	ρ g cm^{-3}	A cm molec^{-1}	Corrected A cm molec^{-1} considering $\rho' = 0.87$ g cm^{-3}	Reference
ν_R	Libration	760	13.2	10	1.32	1	2.8×10^{-17}	3.2×10^{-17}	Hudgins et al. 1993
		750[a]	13.3	10	[a]	[a]	2.6×10^{-17}	2.8×10^{-17}	d'Hendecourt & Allamandola 1986
		760[a]	13.2	14	[a]	[a]	3.10×10^{-17}	3.30×10^{-17}	Gerakines et al. 1995
		763	13.1	25	1.29	1.10	2.5×10^{-17}	3.2×10^{-17}	Mastrapa et al. 2009
ν_2	Bend.	1657	6.035	10	1.32	1	1.0×10^{-17}	1.1×10^{-17}	Hudgins et al. 1993
		1670[a]	5.988	10	[a]	[a]	8.40×10^{-18}	9.1×10^{-18}	d'Hendecourt & Allamandola 1986
		1660[a]	6.024	14	[a]	[a]	1.20×10^{-17}	1.30×10^{-17}	Gerakines et al. 1995
		1666	6.002	25	1.29	1.10	9.5×10^{-18}	1.2×10^{-17}	Mastrapa et al. 2009
		1659	6.028	25	1.27 ± 0.02	0.87 ± 0.03	9.0×10^{-18}	9.0×10^{-18}	This work
$\nu_2 + \nu_R$		2202	4.541	10	1.32	1	3.3×10^{-18}	3.8×10^{-18}	Hudgins et al. 1993
		2209	4.527	25	1.29	1.10	4.3×10^{-18}	5.4×10^{-18}	Mastrapa et al. 2009
ν_1	s-str.	3298	3.032	10	1.32	1	1.7×10^{-16}	2.0×10^{-16}	Hudgins et al. 1993
ν_3	a-str.	3257	3.070	10	1.26	0.94	2.0×10^{-16}	2.2×10^{-16}	Hagen et al. 1981
		3275[a]	3.053	10	[a]	[a]	2.0×10^{-16}	2.2×10^{-16}	d'Hendecourt & Allamandola 1986
		3280[a]	3.049	14	[a]	[a]	2.0×10^{-16}	2.2×10^{-16}	Gerakines et al. 1995
		3285	3.044	25	1.29	1.1	1.9×10^{-16}	2.4×10^{-16}	Mastrapa et al. 2009
		3297	3.033	25	1.27 ± 0.02	0.87 ± 0.03	1.5×10^{-16}	1.5×10^{-16}	This work

[a]d'Hendecourt & Allamandola (1986) and Gerakines et al. (1995) performed measurements using the band strength of the OH-stretching mode of 2×10^{-16} cm molecule^{-1} determined by Hagen et al. (1981) as a reference. So, we consider a density of $\rho = 0.94$ g cm^{-3} used by Hagen et al. (1981) to scale the band strengths found by d'Hendecourt & Allamandola (1986) and Gerakines et al. (1995) using the formula (6).

Table 4. Assignments and band strengths of CO_2 ice.

Label	Mode	Position cm^{-1}	Wavelength μm	T K	n	ρ g cm^{-3}	A cm molec^{-1}	Corrected A cm molec^{-1} considering $\rho' = 1.11$ g cm^{-3}	Reference
ν_2	bend.	660, 665	15.2, 15.3	10	1.22	1	2.0×10^{-17}	1.8×10^{-17}	Hudgins et al. 1993
		660, 655[b]	15.2, 15.3	~ 70	1.41[b]	1.64	1.3×10^{-17}	1.9×10^{-17}	Yamada & Person 1964
		660, 665[a]	15.2, 15.3	14	[a]	[a]	1.1×10^{-17}	1.6×10^{-17}	Gerakines et al. 1995
		660, 665	15.2, 15.3	25	1.27 ± 0.02	1.11 ± 0.03	1.2×10^{-17}	1.2×10^{-17}	This work
ν_3	a-str.	2283[a]	4.380	14	[a]	[a]	7.80×10^{-17}	1.15×10^{-16}	Gerakines et al. 1995
	$^{13}CO_2$	2283[c]	4.380	25	1.27 ± 0.02	1.11 ± 0.03	6.8×10^{-17}	6.8×10^{-17}	This work
ν_3	a-str.	2342	4.270	10	1.22	1	1.4×10^{-16}	1.3×10^{-16}	Hudgins et al. 1993
	$^{12}CO_2$	2342	4.270	~ 70	1.41[b]	1.64	7.6×10^{-17}	1.1×10^{-16}	Yamada & Person 1964
		2343[a]	4.268	14	[a]	[a]	7.60×10^{-17}	1.1×10^{-16}	Gerakines et al. 1995
		2343	4.268	25	1.27 ± 0.02	1.11 ± 0.03	7.6×10^{-17}	7.6×10^{-17}	This work
$2\nu_2 + \nu_3$	comb.	3600	2.778	10	1.22	1	7.9×10^{-19}	7.1×10^{-19}	Hudgins et al. 1993
		3600[a]	2.778	14	[a]	[a]	4.5×10^{-19}	6.6×10^{-19}	Gerakines et al. 1995
		3600	2.778	25	1.27 ± 0.02	1.11 ± 0.03	5.5×10^{-19}	5.5×10^{-19}	This work
$\nu_1 + \nu_3$	comb.	3708	2.697	10	1.22	1	2.6×10^{-18}	2.3×10^{-18}	Hudgins et al. 1993
		3708[a]	2.697	14	[a]	[a]	1.4×10^{-18}	2.1×10^{-18}	Gerakines et al. 1995
		3708	2.697	25	1.27 ± 0.02	1.11 ± 0.03	1.8×10^{-18}	1.8×10^{-18}	This work

[a]Gerakines et al. (1995) performed relative measurements using the integrated cross-section of the stretching mode at 2343 cm^{-1} of 7.6×10^{-17} cm molecule^{-1} determined by Yamada & Person (1964) as a reference. Thus, we used a density of $\rho = 1.64$ g cm^{-3} as used by Yamada & Person (1964) to scale the values of Gerakines et al. (1995) using the formula (6).
[b]The refractive index used by Yamada & Person (1964) is measured in the infrared.
[c]A terrestrial isotopic ratio of ^{12}C / $^{13}C = 92$ has been used to calculate the band strengths of $^{13}CO_2$.

as well as Hudgins et al. (1993) used a density of 1 g cm^{-3} which does not correspond to the reality. Thus, for all the molecules presented below, we have recalculated the band strengths using the recommended densities from Table 2. Indeed, the band strength A and the density ρ are inversely proportional:

$$A' = A \times (\rho/\rho'), \quad (6)$$

where A' is the corrected value, A is literature value, ρ is the density used in the literature and ρ' is the value indicated in Table 2.

The main sources of uncertainties in this study are related to the integration boundaries and the subtraction of the baseline, which lead to an uncertainty of about 20 per cent.

4.1 H_2O (water)

The IR spectrum of pure H_2O ice at 25 K is presented in Fig. 4. The most intense features are due to the stretching modes, the bending mode and the libration mode, respectively, at about 3300 cm^{-1}, 1660 cm^{-1} and 760 cm^{-1}. We also observe features at 3719 and

Table 5. Assignments and band strengths of CO ice.

Label	Mode	Position cm^{-1}	Wavelength μm	T K	n	ρ g cm^{-3}	A cm $molec^{-1}$	Corrected A cm $molec^{-1}$ considering $\rho' = 0.80$ g cm^{-3}	Reference
1–0	str.	2092[a]	4.780	14	[a]	[a]	1.3×10^{-17}	1.7×10^{-17}	Gerakines et al. 1995
	^{13}CO	2092	4.780	25	1.25 ± 0.03	0.8 ± 0.01	1.32×10^{-17}	1.32×10^{-17}	This work
1–0	str.	2138[c]	4.677	30	1.35[c]	1.0288[c]	1.1×10^{-17}	1.4×10^{-17}	Jiang et al. 1975
	^{12}CO	2139[a]	4.675	14	[a]	[a]	1.1×10^{-17}	1.4×10^{-17}	Gerakines et al. 1995
		2139	4.675	25	1.25 ± 0.03	0.8 ± 0.01	1.12×10^{-17}	1.12×10^{-17}	This work
2–0	comb.	4252[b]	2.352	10	[b]	[b]	1.60×10^{-19}	2.1×10^{-19}	Gerakines et al. 2005
	^{12}CO	4253	2.351	25	1.25 ± 0.03	0.8 ± 0.01	1.04×10^{-19}	1.04×10^{-19}	This work

[a]Gerakines et al. (1995) performed relative measurements using the band strength of the 1–0 mode of 1.1×10^{-17} cm $molecule^{-1}$ determined by Jiang et al. (1975) as a reference. Thus to scale this value using the formula 6, we have considered a density of $\rho = 1.0288$ g cm^{-3} used by Jiang et al. (1975). Moreover, to calculate the band strength of ^{13}CO, Gerakines et al. (1995) used a terrestrial isotopic ratio $^{12}C/^{13}C = 89$.
[b]Gerakines et al. (2005) performed relative measurements using the band strength of the 1–0 band of ^{13}CO (1.30×10^{-17} cm $molec^{-1}$) determined by Gerakines et al. (1995) as a reference. To scale this value, we have considered a density of 1.0288 g cm^{-3}.
[c]The measurements of Jiang et al. (1975) correspond to the α-phase at 30 K and the refractive index is for 1000 cm^{-1}.

Table 6. Assignments and band strengths of CH_4 ice. The assignments are according to Brunetto et al. (2008) and Quirico & Schmitt (1997).

Label	Mode	Position cm^{-1}	Wavelength μm	T K	n	ρ g cm^{-3}	A cm $molec^{-1}$	Corrected A cm $molec^{-1}$ considering $\rho = 0.45$ g cm^{-3}	Reference
ν_4	Bend.	1302 + 1297	7.680 + 7.710	10	ND	1	6.1×10^{-18}	1.4×10^{-17}	d'Hendecourt & Allamandola 1986
		1301	7.686	10	1.33	1	3.8×10^{-18}	8.4×10^{-18}	Hudgins et al. 1993
		1302[a]	7.680	10	[a]	0.52[a]	7.3×10^{-18}	8.4×10^{-18}	Boogert et al. 1997
		1302	7.680	12.5	ND	0.52	6.4×10^{-18}	7.4×10^{-18}	Mulas et al. 1998
		1302	7.680	25	1.34 ± 0.04	0.45 ± 0.03	8.0×10^{-18}	8.0×10^{-18}	This work
$\nu_2 + \nu_4$	Comb.	2815.2	3.5523	14	1.329	0.403	2.76×10^{-19}	2.47×10^{-19}	Brunetto et al. 2008
		2816	3.551	25	1.34 ± 0.04	0.45 ± 0.03	3.1×10^{-19}	3.1×10^{-19}	This work
ν_3	Stretch.	3010	3.322	10	ND	1	6.4×10^{-18}	1.4×10^{-17}	d'Hendecourt & Allamandola 1986
		3009	3.323	10	1.33	1	5.7×10^{-18}	1.27×10^{-17}	Hudgins et al. 1993
		3010	3.322	12.5	ND	0.52	9.5×10^{-18}	1.1×10^{-17}	Mulas et al. 1998
		3010	3.322	25	1.34 ± 0.04	0.45 ± 0.03	1.1×10^{-17}	1.1×10^{-17}	This work
$\nu_1 + \nu_4$	Comb.	4202[b]	2.380	10	[b]	[b]	1.60×10^{-18}		Gerakines et al. 2005
		4202.7	2.3794	14	1.329	0.403	3.59×10^{-19}	3.22×10^{-19}	(Brunetto et al. 2008)
		4202	2.380	25	1.34 ± 0.04	0.45 ± 0.03	3.5×10^{-19}	3.5×10^{-19}	This work
$\nu_3 + \nu_4$	Comb.	4300[b]	2.326	10	[b]	[b]	3.40×10^{-18}		Gerakines et al. 2005
		4301.3	2.3249	14	1.329	0.403	6.85×10^{-19}	6.13×10^{-19}	Brunetto et al. 2008
		4301	2.325	25	1.34 ± 0.04	0.45 ± 0.03	5.3×10^{-19}	5.3×10^{-19}	This work
$\nu_2 + \nu_3$	Comb.	4528[b]	2.208	10	[b]	[b]	4.50×10^{-19}		Gerakines et al. 2005
		4528.4	2.2083	14	1.329	0.403	6.52×10^{-20}	5.84×10^{-20}	Brunetto et al. 2008
		4529	2.208	25	1.34 ± 0.04	0.45 ± 0.03	6.6×10^{-20}	6.6×10^{-20}	This work

Note. ND means not defined in the literature.
[a]Boogert et al. (1997) performed a correction of Hudgins et al. (1993)'s band strength using $\rho = 0.52$ g cm^{-3} found by Landolt & Börnstein (1971).
[b]Gerakines et al. (2005) performed relative measurements using a band strength of 1.9 10^{-18} cm $molecule^{-1}$ for the feature at 2815 cm^{-1} as a reference. This latter value was obtained by scaling the intensity of the ν_4 mode at 1306 cm^{-1}. As no density is indicated, we do not scale the values measured by Gerakines et al. (2005) to a density of $\rho' = 0.45$ g cm^{-3}.

3697 cm^{-1}, which correspond, respectively, to the O–H dangling mode of the two- and three-coordinate surface water molecules. These two bands are a typical porosity signature (Rowland & Devlin 1991; Rowland, Fisher & Devlin 1991) which justifies the use of a density value lower than 0.94 g cm^{-3} (see Section 3.1).

Our results are compared with the previous determination of the band strengths of H_2O ice in Table 3. Note that the spectra of Hagen, Tielens & Greenberg (1981), d'Hendecourt & Allamandola (1986) and Mastrapa et al. (2009) do not exhibit the dangling modes. Thus, their sample of H_2O ices was not as porous as ours. As we could not observe the whole libration band, we did not calculate its band strength. For the bending and stretching modes, our value is significantly lower than the results from the literature. This could be due to the porosity of our sample but it is not possible, with our present experimental setup, to directly measure the density and the porosity of our water ice sample. We use a density of 0.87 g cm^{-3} to calculate the band strength but a value as low as 0.65 g cm^{-3} is possible and would lead to a value of 2×10^{-16} cm $molecule^{-1}$ for the stretching mode, comparable with the other reported values. Considering the extremely low value measured by Dohnalek et al. (2003), such a low density value cannot be ruled out. Due to the uncertainty on the porosity, the band strength of porous amorphous water ice cannot be determined with precision. Further works on the absorption of porous amorphous ice are required. Nevertheless, we know that the absorption of porous amorphous water ice seems to decrease with increasing porosity (Cholette et al. 2009).

Concerning compact amorphous water ice, we recommend to use the value of 2.0×10^{-16} cm $molecule^{-1}$ given by Hagen et al. (1981), which is currently used by the astrophysical community.

4.2 CO_2 (carbon dioxide)

The solid IR spectrum of CO_2 ice at 25 K is shown in Fig. 5. The two most intense features are the fundamental modes ν_3 (2343 cm^{-1})

Table 7. Assignments and band strengths of NH_3 ice.

Label	Mode	Position cm^{-1}	Wavelength μm	T K	n	ρ g cm^{-3}	A cm $molec^{-1}$	Corrected A cm $molec^{-1}$ considering $\rho = 0.74$ g cm^{-3}	Reference
ν_2	Umbrella	1070	9.346	10	ND	1	1.7×10^{-17}	2.1×10^{-17}	d'Hendecourt & Allamandola 1986
		1070[a]	9.346	10	[a]	[a]	1.7×10^{-17}	2.1×10^{-17}	Sandford & Allamandola 1993
		1069	9.355	25	1.41 ± 0.04	0.74 ± 0.02	1.63×10^{-17}	1.63×10^{-17}	This work
ν_4	Def.	1624[a]	6.158	10	[a]	[a]	4.7×10^{-18}	5.6×10^{-18}	Sandford & Allamandola 1993
		1630	6.135	25					This work
ν_1	s-str.	3375	2.963	10	ND	1	2.2×10^{-17}	3.0×10^{-17}	d'Hendecourt & Allamandola 1986
ν_3	a-str.	3376	2.962	25	1.41 ± 0.04	0.74 ± 0.02	2.3×10^{-17}	2.3×10^{-17}	This work

Note. ND means not reported in the literature.
[a]Sandford & Allamandola (1993) performed relative measurements using the band strength of the ν_2 umbrella mode at 1070 cm^{-1} of 1.7×10^{-17} cm $molecule^{-1}$ determined by d'Hendecourt & Allamandola (1986) as a reference. So, we consider a density $\rho = 1$ g cm^{-3} as used by d'Hendecourt & Allamandola (1986) to scale the band strength found by Sandford & Allamandola (1993).

Table 8. Assignments and band strengths of CH_3OH ice.

Label	Mode	Position cm^{-1}	Wavelength μm	T K	n	ρ g cm^{-3}	A cm $molec^{-1}$	Corrected A cm $molec^{-1}$ considering $\rho' = 1.01$ g cm^{-3}	Reference
ν_{12}	Torsion	694	14.41	10	1.33	1	1.4×10^{-17}		Hudgins et al. 1993
		700	14.29	10	ND	1	1.6×10^{-17}		d'Hendecourt & Allamandola 1986
ν_8	CO str.	1026	9.747	10	1.33	1	1.80×10^{-17}	1.78×10^{-17}	Hudgins et al. 1993
		1026	9.747	10	ND	1	1.80×10^{-17}	1.78×10^{-17}	d'Hendecourt & Allamandola 1986
		1034	9.671	10	ND	ND	1.30×10^{-17}		Palumbo et al. 1999
		1031	9.699	25	1.33 ± 0.04	1.01 ± 0.03	1.07×10^{-17}	1.07×10^{-17}	This work
ν_{11}	CH_3 rock	1130	8.850	10	1.33	1	1.80×10^{-18}	1.78×10^{-18}	Hudgins et al. 1993
		1124	8.897	10	ND	1	1.30×10^{-18}	1.29×10^{-18}	d'Hendecourt & Allamandola 1986
		1129	8.857	10	ND	ND	1.50×10^{-18}		Palumbo et al. 1999
		1129	8.857	25	1.33 ± 0.04	1.01 ± 0.03	1.40×10^{-18}	1.40×10^{-18}	This work
ν_5	CH_3 s-bend.	1460[a]	6.849	10	1.33	1	1.20×10^{-17a}	1.19×10^{-17}	Hudgins et al. 1993
ν_4	CH_3 a-bend.	1460[a]	6.849	10	ND	1.00	1.00×10^{-17a}	9.90×10^{-18}	d'Hendecourt & Allamandola 1986
ν_{10}	OH bend.	1460[a]	6.849	10	ND	ND	9.1×10^{-18a}		Palumbo et al. 1999
ν_6	CH_3 a-bend.	1459[a]	6.854	25	1.33 ± 0.04	1.01 ± 0.03	6.55×10^{-18a}	6.55×10^{-18}	This work
	comb.	2526	3.959	10	1.33	1	2.80×10^{-18}	2.77×10^{-18}	Hudgins et al. 1993
		2527	3.957	25	1.33 ± 0.04	1.01 ± 0.03	1.78×10^{-18}	1.78×10^{-18}	This work
ν_3	CH_3 s-str.	2700- 3600[b]	3.704–2.778[b]	10	1.33	1	1.60×10^{-16b}	1.58×10^{-16}	Hudgins et al. 1993
ν_9	CH_3 a-str.	2700- 3600[b]	3.704–2.778[b]	10	ND	1	1.39×10^{-16b}	1.37×10^{-16}	d'Hendecourt & Allamandola 1986
ν_1	OH str.	2700- 3600[b]	3.704–2.778[b]	10	ND	ND	1.28×10^{-16b}		Palumbo et al. 1999
		2700–3600[b]	3.704–2.778[b]	25	1.33 ± 0.04	1.01 ± 0.03	1.01×10^{-16b}	1.01×10^{-16}	This work

Note. ND means not defined in the literature.
[a]The entire band located between 1300 and 1550 cm^{-1} is composed of four different modes.
[b]The entire band between 2700 and 3600 cm^{-1} is due to three different modes. The band strength is derived from the integration of the whole band or from the addition of the band strengths for the three individual modes.

and ν_2 (600–665 cm^{-1}) corresponding, respectively, to the asymmetric stretching and bending modes. We also observe some combination modes at 3600 and 3708 cm^{-1} as well as a fundamental mode of the isotopic $^{13}CO_2$ at 2283 cm^{-1} (Fig. 5).

Our results for the band strengths of CO_2 ice are compared with previous results in Table 4. Our band strengths are significantly lower than those of Hudgins et al. (1993) even if we consider the rescaled values using a higher density (i.e. $\rho' = 1.11$ g cm^{-3}). The measurements of Yamada & Person (1964) have been performed between 65 and 80 K using a density of 1.64 g cm^{-3}. This last value is in agreement with the measurements of Schulze & Abe (1980), Wood & Roux (1982) and Satorre et al. (2008) in the same temperature range. Since the density and the refractive index of CO_2 ice depend on the temperature, we compare our measurements directly with the initial values of Yamada & Person (1964). Both measurements present an excellent agreement for the fundamental bands of $^{12}CO_2$. Compared to Gerakines et al. (1995), our A-values are 25 per cent lower for the combination modes at 3600 and 3708 cm^{-1} of $^{12}CO_2$ and for the fundamental mode at 2283 cm^{-1} of $^{13}CO_2$. This difference could be due to saturation of the 2343 cm^{-1} mode which was used as a reference by Gerakines et al. (1995).

4.3 CO (carbon monoxide)

The IR spectrum of pure CO ice at 25 K is shown in Fig. 6. The most intense feature is the 1–0 fundamental mode (2139 cm^{-1}). We also observe a combination mode at 4253 cm^{-1} as well as a fundamental mode of ^{13}CO at 2092 cm^{-1} (see Fig. 6 and Table 5).

Table 9. Assignments and band strengths of HCOOH ice.

Label	Mode	Position cm^{-1}	Wavelength μm	T K	A cm molec^{-1}	Reference
ν_5	OH bend.	929	10.76	25	6.4×10^{-17}	This work
ν_8	CH bend.	1074	9.311	25	3.1×10^{-19}	This work
ν_6	CO str.	1216	8.224	25	2.9×10^{-17}	This work
ν_5	OH bend.	1380[a]	7.246	10	2.6×10^{-18}[a]	Schutte et al. 1999
ν_4	CH bend.	1384	7.225	25	3.7×10^{-18}	This work
ν_3	C=O str.	1710[a]	5.848	10	6.7×10^{-17}[a]	Schutte et al. 1999
		1708	5.855	25	5.4×10^{-17}	This work
ν_1	OH str.	2586	3.867	25	1.4×10^{-16}	This work
ν_2	CH str.	2757	3.627			
		2939	3.403			

[a]Schutte et al. (1999) relative measurements considering the band strength of the stretching C=O mode at 1710 cm^{-1} obtained in the gas phase by Marechal (1987) as a reference.

Table 10. Assignments and band strengths of H_2CO ice at 25 K. The assignments are according to Nelander (1980).

Label	Mode	Position cm^{-1}	Wavelength μm	T K	A cm molec^{-1}	Reference
ν_4	CH_2 wag.	1177	8.496	10	4.8×10^{-19}	Schutte et al. 1993
		1178	8.489	25	7.2×10^{-19}	This work
ν_6	CH_2 rock.	1244	8.039	10	1.0×10^{-18}	Schutte et al. 1993
		1247	8.019	25	1.5×10^{-18}	This work
ν_3	CH_2scis.	1494	6.693	10	3.9×10^{-18}	Schutte et al. 1993
		1500	6.667	25	5.1×10^{-18}	This work
ν_2	C=O str.	1723	5.804	10	9.6×10^{-18}	Schutte et al. 1993
		1725	5.797	25	1.6×10^{-17}	This work
ν_1	CH_2 s-str.	2822	3.544	10	3.7×10^{-18}	Schutte et al. 1993
		2829	3.535	25	1.3×10^{-17}	This work
ν_5	CH_2 a-str.	2883	3.469	10	2.8×10^{-18}	Schutte et al. 1993
		2891	3.459	25	4.7×10^{-18}	This work
$\nu_2 + \nu_6$	comb.	2991	3.343	10	1.4×10^{-18}	Schutte et al. 1993
		2997	3.337	25	3.2×10^{-18}	This work

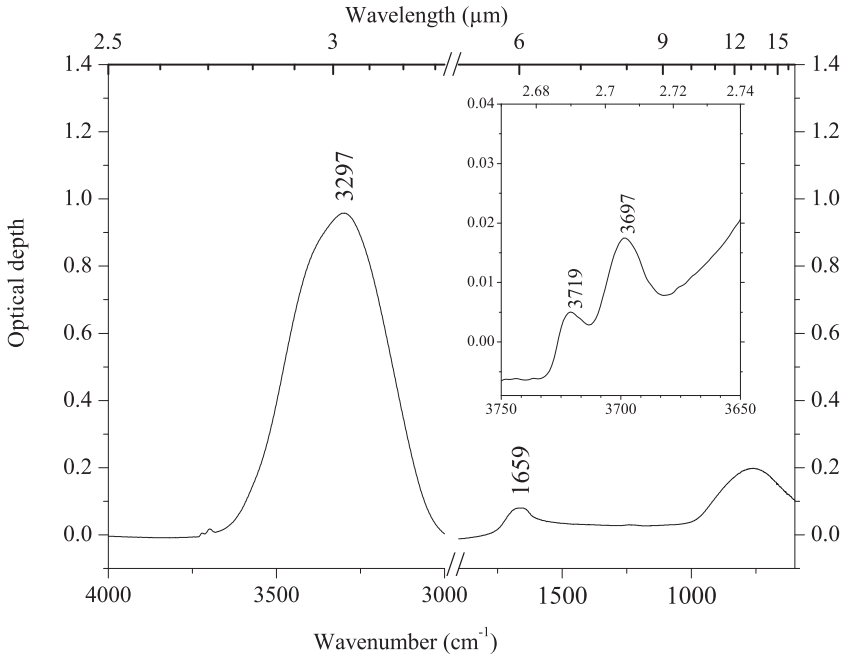

Figure 4. IR spectrum of H_2O ice at 25 K for a thickness of 0.76 μm corresponding to a column density of 2.2×10^{18} molecules cm^{-2}. The deposition rate was 2.3×10^{15} molecules cm^{-2} s^{-1}.

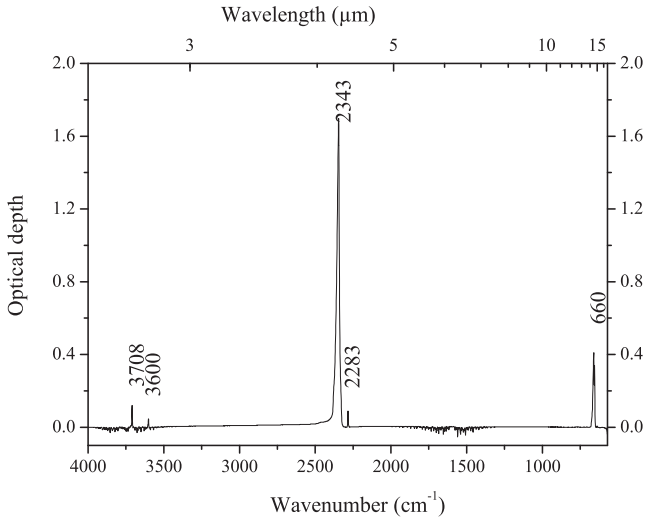

Figure 5. IR spectrum of CO_2 ice at 25 K for a thickness of 0.37 μm corresponding to a column density of 6.5×10^{17} molecules cm^{-2}. The deposition rate was 4×10^{14} molecules cm^{-2} s^{-1}.

Our measured band strengths of CO ice are presented in Table 5 together with the results from previous studies. We found only one publication (Jiang et al. 1975) presenting an absolute measurement of the band strength of the 1–0 band. In that study, CO films were formed at 30 K and the thickness was retrieved from the interference pattern using a refractive index of 1.36 and a density of 1.0288 g cm^{-3} corresponding to the crystalline α-phase of solid CO (Vegard 1930). The band strength of Jiang et al. (1975) has been used as a reference by Gerakines et al. (1995) to scale the relative intensity measurement of the 1–0 band of ^{13}CO (see Table 5).

Using the recommended density (i.e. $\rho' = 0.80$ g cm^{-3}; see Table 2), we recalculate the band strength measured by Jiang et al. (1975) and find a value which is 25 per cent higher than ours. A possible explanation for this discrepancy could be the value of the refractive index that Jiang et al. (1975) used is about 10 per cent higher than the one recently measured by Baratta & Palumbo (1998). Thus, Jiang et al. (1975) could have overestimated their band strength by 10 per cent reducing to only 15 per cent the difference with our value.

For the 1–0 band of ^{13}CO, our band strength is 25 per cent lower than Gerakines et al.'s (1995). This difference is identical to the 1–0 band of ^{12}CO which has been used as a reference by Gerakines et al. (1995).

To measure the band strength of the weak 2–0 overtone band, Gerakines et al. (2005) used the 1–0 band of ^{13}CO as a reference and found a value two times stronger than ours. We suspect that the rescaling made by Gerakines et al. (2005) has not been done properly for CO.

For the 1–0 mode of ^{12}CO, we recommend a band strength of 1.1×10^{-17} cm molecule^{-1} which corresponds also to the initial value of Jiang et al. (1975) without rescaling process. Note that numerous authors already commonly use this value.

4.4 CH_4 (methane)

The IR spectrum of CH_4 ice at 25 K is shown in Fig. 7. The two most intense features are the fundamental modes ν_4 (1302 cm^{-1}) and ν_3 (3010 cm^{-1}) corresponding, respectively, to the deformation and stretching of the C–H bonds. Numerous combination bands are also observed with lower intensity at 2816, 4202, 4301 and 4529 cm^{-1}.

Our results as well as previous measurements of the band strengths of CH_4 ice are presented in Table 6. Among the absolute measurements, only Hudgins et al. (1993) and Brunetto et al. (2008) have specified the refractive indices used, i.e. 1.33 and 1.329 in close agreement with the value that we recommend (see

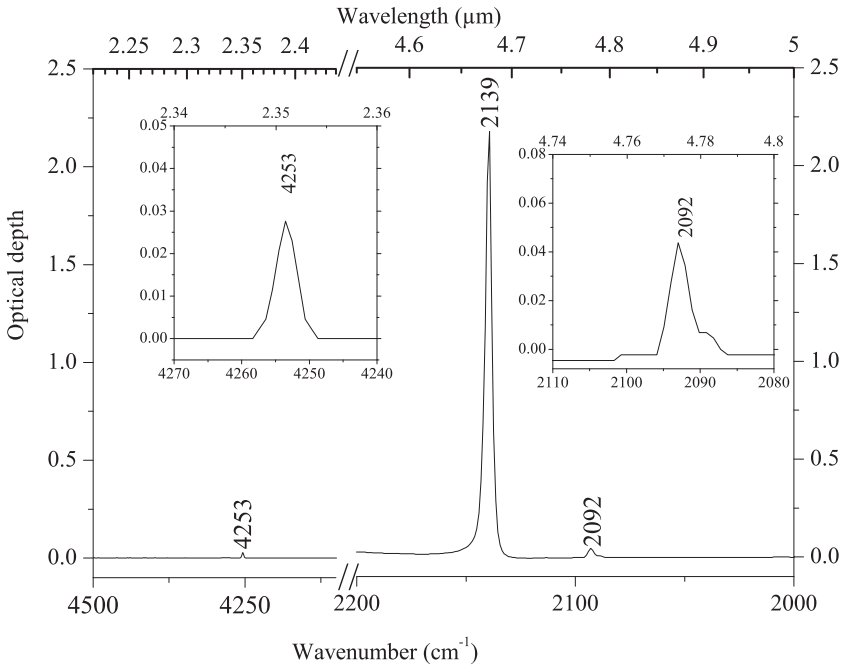

Figure 6. IR spectrum of CO ice at 25 K for a thickness of 0.74 μm corresponding to a column density of 1.3×10^{18} molecules cm^{-2}. The deposition rate was 2×10^{15} molecules cm^{-2} s^{-1}.

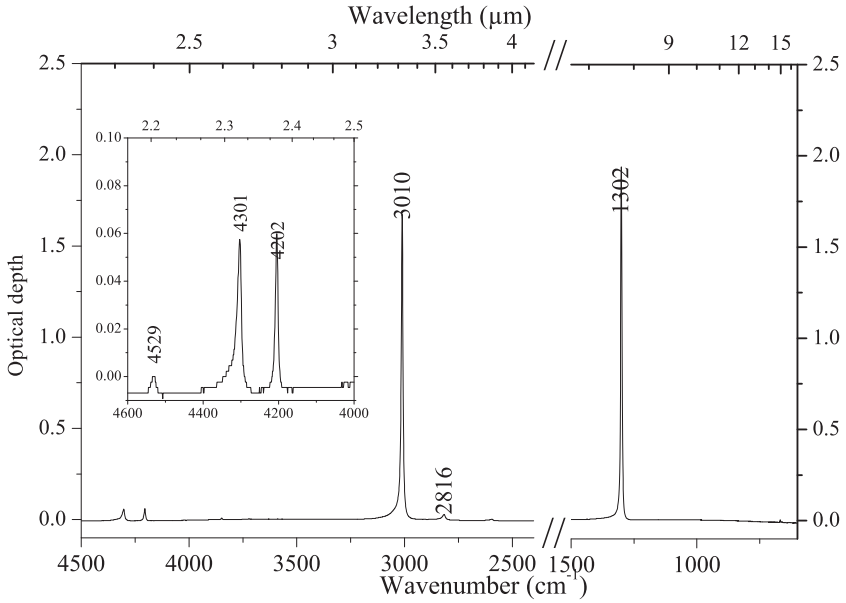

Figure 7. IR spectrum of CH_4 ice at 25 K for a thickness of 1.12 μm corresponding to a column density of 1.8×10^{18} molecules cm^{-2}. The deposition rate was 2.3×10^{15} molecules cm^{-2} s^{-1}.

Table 2). Recalculating the band strengths of Hudgins et al. (1993) and Mulas et al. (1998) with a density of $\rho' = 0.45$ g cm^{-3} gives a good agreement ($\pm$ 10 per cent) with our value for the ν_4 fundamental mode. A reasonable agreement is also obtained for the ν_3 fundamental mode. On the other side, the values of d'Hendecourt & Allamandola (1986) are larger than ours for both fundamental modes. Concerning the combination modes, we observe differences up to 20 per cent with the values of Brunetto et al. (2008) and a very large difference with Gerakines et al. (2005). But as already discussed by Brunetto et al. (2008), the results obtained by Gerakines et al. (2005) are doubtful.

Finally for CH_4, we retain the very good agreement of our measurements with Hudgins et al. (1993) and Mulas et al. (1998) for the fundamental modes using our recommended density value of $\rho' = 0.45$ g cm^{-3}. Note that the band strengths are slightly higher than the values found by Boogert et al. (1997) which are currently used by astrophysical community and derived from the measurements of Hudgins et al. (1993).

4.5 NH_3 (ammonia)

The IR spectrum of pure NH_3 ice at 25 K is shown in Fig. 8. The observed bands are due to the fundamental modes ν_2 (1069 cm^{-1}), ν_4 (1630 cm^{-1}), ν_1 (3202 cm^{-1}) and ν_3 (3376 cm^{-1}).

Table 7 presents our measured band strengths of NH_3 and the values found in the literature. The large absorption between 3100 and 3500 cm^{-1} is due to the overlapping asymmetric (ν_3) and symmetric (ν_1) N–H stretching modes. Since these modes cannot be resolved we have integrated the whole feature to determine the band strength. The band corresponding to the deformation mode (ν_4) presents a very long wing towards shorter wavenumber which makes the definition of the integration limits very difficult and thus no band strength has been calculated for this mode.

Comparing with the only publication (d'Hendecourt & Allamandola 1986) reporting absolute measurements we found a very good agreement for the band strengths. But the values diverge when applying the recommended ice density.

4.6 CH_3OH (methanol)

The IR spectrum of pure CH_3OH ice at 25 K is shown in Fig. 9. In Table 8, we list the observed absorption bands. CH_3 and OH bending modes overlap and cannot be distinguished around 1460 cm^{-1} in pure solid phase. The entire absorption between 2700 and 3600 cm^{-1} is due to three different stretching modes of CH_3 and OH. Therefore, we chose to integrate the whole absorption system between 2700 and 3600 cm^{-1}.

Our results for the band strengths of CH_3OH ice are presented in Table 8 using the refractive index measured in the liquid phase and the density of the crystalline α-phase. Among the previous absolute measurements, only Hudgins et al. (1993) has specified the refractive index and the density that were used to calculate the column density of their CH_3OH film. Those values are identical to ours, so that both sets of band strengths are directly comparable. Nevertheless, our band strengths are about 40 per cent lower than the values found by Hudgins et al. (1993). We cannot find any explanation for this difference. d'Hendecourt & Allamandola (1986) and Palumbo, Castorina & Strazzulla (1999) did not specify the densities and refractive indices used to calculate the column densities of their films but their band strengths are intermediate between ours and Hudgins et al. (1993) values.

4.7 HCOOH (formic acid)

The IR spectrum of pure HCOOH ice at 25 K is shown in Fig. 10. It is very similar to the spectrum obtained by Bisschop et al. (2007). The observed features are indicated in Fig. 10 and their assignments are given in Table 9.

No absolute measurements of pure ice film of HCOOH at low temperature are available in the literature. A summary of previous estimated values in the gas phase, in solid phase diluted in H_2O and by theoretical calculations is given in Table 3 of Bisschop

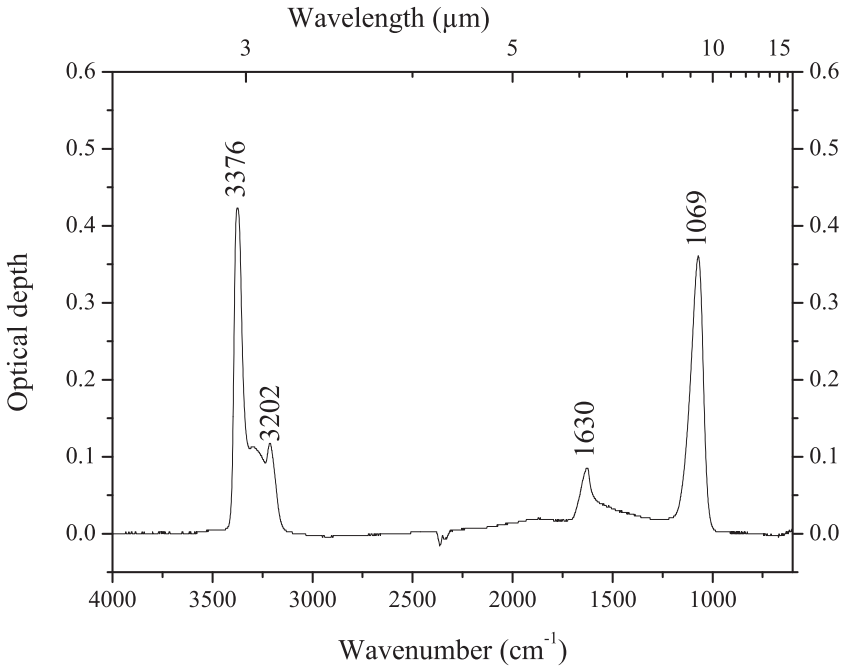

Figure 8. IR spectrum of NH_3 ice at 25 K for a thickness of 0.65 μm corresponding to a column density of 1.7×10^{18} molecules cm^{-2}. The deposition rate was 1.3×10^{15} molecules cm^{-2} s^{-1}.

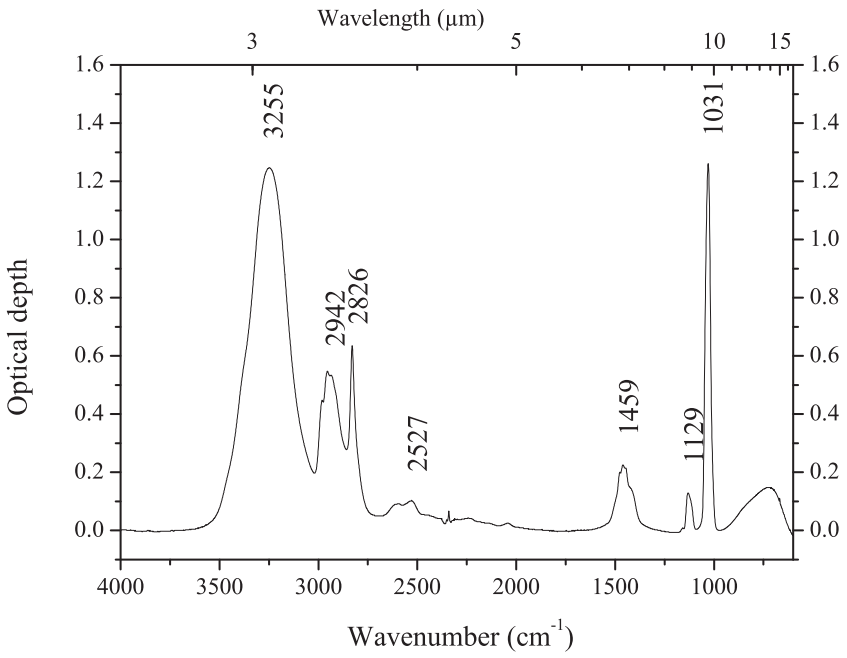

Figure 9. IR spectrum of CH_3OH ice at 25 K for a thickness of 1.9 μm corresponding to a column density of 3.5×10^{18} molecules cm^{-2}. The deposition rate was 2.0×10^{15} molecules cm^{-2} s^{-1}.

et al. (2007). The band strengths currently used in the astrophysical community are those of Schutte et al. (1999) which have been measured relatively to the value of 6.7×10^{-17} cm molecule^{-1} for the stretching C=O mode at 1710 cm^{-1}. The latter value was obtained in the gas phase by Marechal (1987). Table 9 presents our results for pure HCOOH ice together with those of Schutte, Allamandola & Sandford (1993). Comparing the values, we found a band strength 40 per cent higher for the feature around 1380 cm^{-1} and 20 per cent lower at 1708 cm^{-1}. We have also compared our spectrum with the spectrum of Bisschop et al. (2007) and found almost identical relative intensities for the 1380 and 1708 cm^{-1} features. Thus, we are confident in our measurements, and recommend using our new values (Table 9). But the refractive index and the density used to calculate the column density are those of the liquid phase leading to a large uncertainty on the solid phase band strength.

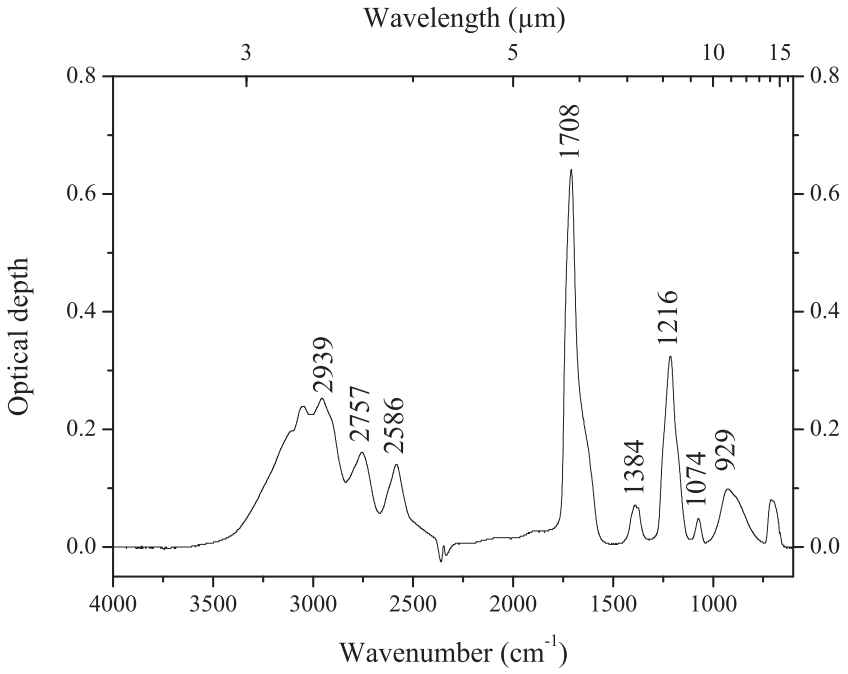

Figure 10. IR spectrum of HCOOH ice at 25 K for a thickness of 0.56 μm corresponding to a column density of 8.9×10^{17} molecules cm^{-2}. The deposition rate was 2.9×10^{15} molecules cm^{-2} s^{-1}.

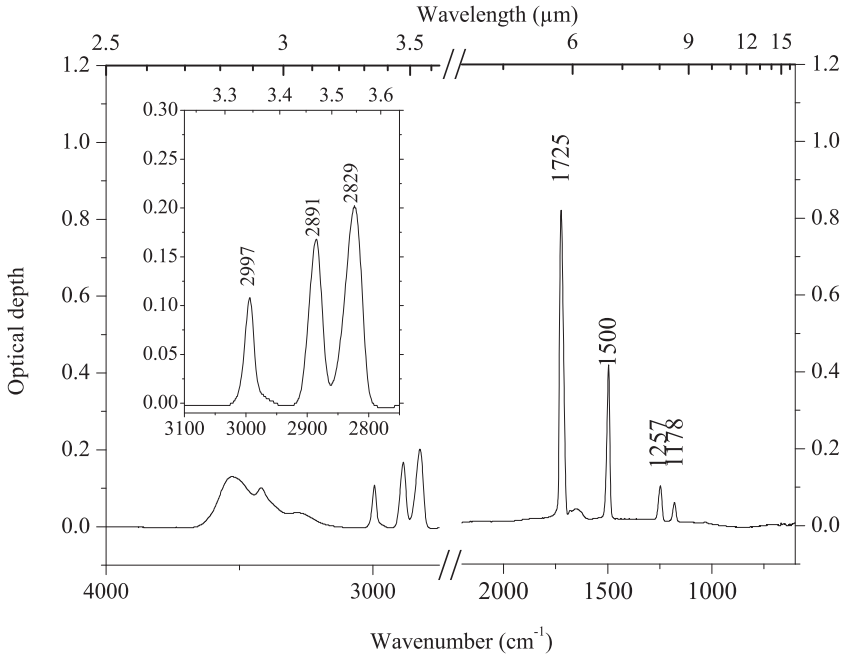

Figure 11. IR spectrum of H_2CO ice at 25 K for a thickness of 1.19 μm corresponding to a column density of 2.4×10^{18} molecules cm^{-2}. The deposition rate was 1.2×10^{15} molecules cm^{-2} s^{-1}.

4.8 H_2CO (formaldehyde)

The IR spectrum of pure H_2CO ice at 25 K is shown Fig. 11. The assignments of the most intense features are given in Table 10.

Schutte et al. (1993) measured solid H_2CO band strengths. The published values were first obtained from a H_2O:H_2CO = 100:3 ice mixture by taking the 760 cm^{-1} libration mode of H_2O as a reference and using the band strength measured by D'Hendecourt & Allamandola (1986). The contribution of pure H_2CO was then derived by scaling the relative areas of the infrared features and assuming that the 1720 cm^{-1} feature has the same band strength in both the pure H_2CO and the H_2O:H_2CO ice mixture. Table 10 presents the measured band strength of pure H_2CO ice. Those values are about 50 per cent higher than previous measurements by Schutte et al. (1993). Such a discrepancy can be explained by the fact that mixing with water often changes the absorption (Kerkhof, Schutte & Ehrenfreund 1999). A large uncertainty remains since we use a density value determined in the

liquid phase and an arbitrary value for the refractive index (see Section 3).

5 DISCUSSION AND ASTROPHYSICAL IMPLICATIONS

Infrared space telescopes such as *ISO* and *Spitzer* allowed the identification of numerous molecules in the icy dust grain mantles of the ISM. Quantifying the observed molecules is essential to understand the physico-chemical evolution of the icy objects.

In this paper, we have determined infrared band strengths for several molecules in pure condensed form at 25 K. Uncertainties are generally better than 10 per cent when the optical indices at visible wavelengths and the densities are well constrained but can be much higher due to the difficulty to determine the column densities of our samples.

For CO_2, CO, CH_4 and NH_3, the densities and the optical indices at visible wavelengths of pure ices films were found in the literature (see Section 3) and seem to be reliable. Using the recommended densities, the band strengths measured for these four molecules are in agreement with previous determinations within 20 per cent uncertainty.

For solid HCOOH, H_2CO and amorphous CH_3OH, the refractive indices and densities have never been measured. For porous amorphous H_2O, we are unable to characterize the porosity. Thus, we cannot determine accurately the band strengths of these four molecules. We find differences with previous determinations up to 50 per cent. For CH_3OH, the comparison of our spectra with Galvez et al. (2009) shows that we formed a low temperature amorphous phase of CH_3OH ice. As the density of this amorphous phase is unknown, we have used the value of the crystalline α-phase. For the porous amorphous water ice, the porosity and thus the density cannot be determined precisely. In that case, the band strengths could be underestimated since the measurements of Cholette et al. (2009) showed that the absorption of water could decrease with increasing porosity. For H_2CO and HCOOH, we used available liquid phase values for optical indices and densities. For H_2CO, the previous measurements were performed in ice mixture dominated by H_2O (Schutte et al. 1993) and for HCOOH only relative measurements using gas phase values as a reference were performed (Schutte et al. 1999). Thus, it is not surprising to find large differences in the literature for H_2CO and HCOOH ices. The lack of knowledge of the optical indices and densities of pure molecules leads to large uncertainties on the band strengths. We recommend to use the band strengths determined in this work, except for H_2O. Indeed, for each molecule, the given band strengths were obtained from four different series of measurements, each one containing more than 50 spectra of the pure molecule. Note that the band strengths do not show any significant deviation in our deposition rate studied range.

Table 11 gathers the band strengths (and their original references) used by Boogert et al. (2008), Pontoppidan et al. (2008), Oberg et al. (2008) and Bottinelli et al. (2010) to calculate molecular abundances from *Spitzer* spectra. For H_2O, CO_2 and CO, pure ice band strengths have been employed by the authors and the comparison with our values is straightforward. For all three molecules, the difference with our values is lower than the measurement uncertainty. For all the other molecules, the band strengths used to retrieve the column densities in the ISM have been measured in mixtures with water. For CH_3OH and NH_3 in water, the band strengths have been measured by Kerkhof et al. (1999) relatively to pure ice films measurements. For NH_3, our recommended value is in agreement with the one of d'Hendecourt & Allamandola (1986; see Section 4.5), which has

Table 11. Comparison between band strengths of main bands advised in this study and the ones that have been used by Boogert et al. (2008), Pontoppidan et al. (2008), Oberg et al. (2008), and Bottinelli et al. (2010) to retrieve quantitatively the column densities of ices.

ice	Mode	Position (cm^{-1})	Wavelength (μm)	Used A (10^{17} cm molecule^{-1})	Observational references	Experimental references	Ice state	Advised A (10^{17} cm molecule^{-1})	% discrepancy
H_2O	a-str.	3333	3.000	20	Boogert et al. 2008	Hagen et al. 1981	pure	20	0
CO_2	Bend	660	15.15	1.10	Pontoppidan et al. 2008	Gerakines et al. (1995) and Yamada & Person (1964)	pure	1.20	+9
CO	str ^{12}CO	2139	4.675	1.10	Pontoppidan et al. 2008	Gerakines et al. 1995	pure	1.12	+2
CH_4	Bend	1302	7.680	0.47	Oberg et al. 2008	Boogert et al. 1997 and Hudgins et al. (1993)	H_2O:CH_4 = 20:1		
CH_3OH	CO stretch	1027	9.737	1.6	Boogert et al. (2008)	Kerkhof et al. 1999	H_2O:CH_3OH = 8.9:1	0.95	−40
NH_3	Umbrella	1069	9.355	1.30	Boogert et al. 2008	Kerkhof et al. 1999	H_2O:NH_3 = 11:1	1.25	−4
HCOOH	OH bend	1379	7.252	0.26	Boogert et al. 2008	Schutte et al. 1999	H_2O:HCOOH = 10:1		
H_2CO	C=O str.	1725	5.797	0.96	Boogert et al. 2008	Schutte et al. 1993	H_2O:H_2CO = 100:3		

been used as a reference by Kerkhof et al. (1999). Thus, our work on NH_3 confirms the actual quantification of this molecule in the ISM. For CH_3OH, our results are 40 per cent lower than previous values obtained by d'Hendecourt & Allamandola (1986) and Hudgins et al. (1993; see Section 4.6) which has been used as a reference by Kerkhof et al. (1999). In this case, the column densities and abundances of CH_3OH, retrieved from the observations could have been overestimated. The experimental procedure used to measure the reference band strengths of CH_4, HCOOH and H_2CO mixed with H_2O does not allow a rescaling process. For those molecules, we cannot directly compare our values with the ones used to calculate the column densities in the ISM. Nevertheless, we have to keep in mind that (i) the density of CH_4 used by Hudgins et al. (1993) was overestimated by a factor of 2 (see section 4.4) (ii) the HCOOH ice band strengths by Schutte et al. (1999) have been determined relatively to gas phase measurements (see Section 4.7) and (iii) the measurements of the H_2CO ice band strengths by Schutte et al. (1993) have been performed in mixtures with water taking the libration mode of water as a reference (see Section 4.8). For all three molecules, we found discrepancies on the band strengths as high as 50 per cent with the values used to retrieve the column densities in the ISM.

The abundances of CH_3OH, CH_4, H_2CO and HCOOH in the ISM could thus be very different than presently thought due to large inaccuracies on the measured band strengths.

6 CONCLUSION

Band strengths are essential to determine column densities from infrared observations in the ISM. We have reviewed refraction indices at visible wavelength, densities and infrared band strengths of pure solid H_2O, CO, CO_2, CH_3OH, NH_3, CH_4, HCOOH and H_2CO. New laboratory values of the *A*-value were determined and compared with the literature. Despite the difficulty to compare measurements done in different experimental conditions, we discuss the reliability of refraction indices, densities and band strengths for pure ices.

For CO_2, CO, CH_4 and NH_3, refraction indices and densities are found in the literature. Band strengths determined in this work are in good agreement with previous determinations within a 20 per cent uncertainty.

For the porous amorphous H_2O ice films, the porosity and density remain largely uncertain leading to very large uncertainties on the band strengths. But the value given by Hagen et al. (1981) seems to be valid for compact amorphous ice. Concerning pure amorphous CH_3OH, H_2CO and HCOOH, the densities and refractive indices are unknown leading to large uncertainties on their band strengths. New determinations are proposed in this work.

For porous amorphous H_2O as well as for CH_3OH, H_2CO and HCOOH, further works are required to diminish the uncertainties. Future works should include simultaneous measurements of the thickness, density and infrared spectra of ices. Such simultaneous measurements are possible with an experimental setup similar to the one used by Wood & Roux (1982) including a quartz-crystal microbalance in conjunction with a dual-angle laser interference technique to measure simultaneously the thickness and the density of the ice film as well as an infrared spectrometer.

Finally, we show that the band strengths used to calculate the column densities and abundances of CH_4, CH_3OH, HCOOH and H_2CO are inaccurate leading to some doubts on the real abundances of these four molecules in the ices of the ISM.

ACKNOWLEDGEMENTS

We would like to acknowledge UPEC (Université Paris-Est Créteil), INSU (Institut National des Sciences de l'Univers), EPOV CNRS program (Environnements Planétaires et Origines de la Vie) and the DIM ACAV (Astrophysique et Conditions d'Apparition de la Vie) for funding in support of the OREGOC experiment. This study was supported by the CNES (Centre National d'Etudes Spatiales), in the framework of the ROSETTA/COSIMA instrument project. We would like also to thank the ESEP Labex (Exploration Spatiale des Environnements Planétaires).

REFERENCES

Baratta G. A., Palumbo M. E., 1998, J. Opt. Soc. Am. A, 15, 3076
Berland B. S., Brown D. E., Tolbert M. A., George S. M., 1995, Geophys. Res. Lett., 22, 3493
Bisschop S. E., Fuchs G. W., Boogert A. C. A., van Dishoeck E. F., Linnartz H., 2007, A&A, 470, 749
Boogert A. C. A. et al., 2008, ApJ., 678, 985
Boogert A. C. A., Schutte W. A., Helmich F. P., Tielens A., Wooden D. H., 1997, A&A, 317, 929
Bottinelli S. et al., 2010, ApJ., 718, 1100
Briani G., Fray N., Cottin H., Benilan Y., Gazeau M. C., Perrier S., 2013, Icarus, 226, 541
Brown D. E., George S. M., Huang C., Wong E. K. L., Rider K. B., Smith R. S., Kay B. D., 1996, J. Phys. Chem., 100, 4988
Brunetto R., Caniglia G., Baratta G. A., Palumbo M. E., 2008, ApJ, 686, 1480
Cholette F., Zubkov T., Smith R. S., Dohnalek Z., Kay B. D., Ayotte P., 2009, J. Phys. Chem. B, 113, 4131
Dartois E., 2005, Space Sci. Rev., 119, 293
Dawes A. et al., 2007, J. Chem. Phys., 126, 244711
d'Hendecourt L. B., Allamandola L. J., 1986, Astron. Astrophys. Suppl. Ser., 64, 453
Dohnalek Z., Kimmel G. A., Ayotte P., Smith R. S., Kay B. D., 2003, J. Chem. Phys., 118, 364
Escribano R. M., Caro G. M. M., Cruz-Diaz G. A., Rodriguez-Lazcano Y., Mate B., 2013, Proc. Natl. Acad. Sci., 110, 12899
Galvez O., Mate B., Martin-Llorente B., Herrero V. J., Escribano R., 2009, J. Phys. Chem. A, 113, 3321
Gerakines P. A., Bray J. J., Davis A., Richey C. R., 2005, ApJ, 620, 1140
Gerakines P. A., Schutte W. A., Greenberg J. M., Vandishoeck E. F., 1995, A&A, 296, 810
Ghormley J. A., Hochanad C. J., 1971, Science, 171, 62
Gibb E. L., Whittet D. C. B., Boogert A. C. A., Tielens A., 2004, ApJS, 151, 35
Hagen W., Tielens A., Greenberg J. M., 1981, Chem. Phys., 56, 367
Hollenberg J., Dows D. A., 1961, J. Chem. Phys., 34, 1061
Hudgins D. M., Sandford S. A., Allamandola L. J., Tielens A., 1993, ApJS, 86, 713
Jiang G. J., Person W. B., Brown K. G., 1975, J. Chem. Phys., 62, 1201
Kerkhof O., Schutte W. A., Ehrenfreund P., 1999, A&A, 346, 990
Landolt H., Börnstein R., 1971, Zahlenwerte und Funktionen aus Physik, Chemie, Astronomie, Geophysik un Technik. Band II. Springer Verlarg, Berlin, p. 944
Le Roy L., Briani G., Briois C., Cottin H., Fray N., Thirkell L., Poulet G., Hilchenbach M., 2012, Planet Space Sci., 65, 83
Loerting T. et al., 2011, Phys. Chem. Chem. Phys., 13, 8783
Marechal Y., 1987, J. Chem. Phys., 87, 6344
Mastrapa R. M., Sandford S. A., Roush T. L., Cruikshank D. P., Ore C. M. D., 2009, ApJ, 701, 1347
Mate B., Galvez O., Herrero V. J., Escribano R., 2009, ApJ, 690, 486
Mulas G., Baratta G. A., Palumbo M. E., Strazzulla G., 1998, A&A, 333, 1025

Narten A. H., 1976, J. Chem. Phys., 64, 1106
Nelander B., 1980, J. Chem. Phys., 73, 1026
Oberg K. I., Boogert A. C. A., Pontoppidan K. M., Blake G. A., Evans N. J., Lahuis F., van Dishoeck E. F., 2008, ApJ, 678, 1032
Oberg K. I., Boogert A. C. A., Pontoppidan K. M., van den Broek S., van Dishoeck E. F., Bottinelli S., Blake G. A., Evans N. J., 2011, ApJ, 740, 109
Palumbo M. E., Castorina A. C., Strazzulla G., 1999, A&A, 342, 551
Pipes J. G., Roux J. A., Smith A. M., Scott H. E., 1978, AIAA J., 16, 984
Pontoppidan K. M. et al., 2008, ApJ, 678, 1005
Quirico E., Schmitt B., 1997, Icarus, 128, 181
Romanescu C., Marschall J., Kim D., Khatiwada A., Kalogerakis K. S., 2010, Icarus, 205, 695
Roux J. A., Wood B. E., Smith A. M., Plyler R. R., 1980, Arnold Engineering Development Center Int. Rep. AEDC-TR-79, AEDC, Arnold Air Force Base
Rowland B., Devlin J. P., 1991, J. Chem. Phys., 94, 812
Rowland B., Fisher M., Devlin J. P., 1991, J. Chem. Phys., 95, 1378
Sandford S. A., Allamandola L. J., 1993, ApJ, 417, 815
Satorre M. A., Domingo M., Millan C., Luna R., Vilaplana R., Santonja C., 2008, Planet Space Sci., 56, 1748
Satorre M. A., Leliwa-Kopystynski J., Santonja C., Luna R., 2013, Icarus, 225, 703
Schulze W., Abe H., 1980, Chem. Phys., 52, 381
Schutte W. A., Allamandola L. J., Sandford S. A., 1993, Icarus, 104, 118
Schutte W. A. et al., 1999, A&A, 343, 966
Seiber B. A., Wood B. E., Smith A. M., Muller P. R., 1970, Science, 170, 652
Torrie B. H., Binbrek O. S., Strauss M., Swainson I. P., 2002, J. Solid State Chem., 166, 415
Vegard L., 1930, Z. Phys., 61, 185
Warren S. G., 1986, Appl. Opt., 25, 2650
Weast R. C., Astle M. J., 1985, CRC Handbook of Data on Organic Compounds. CRC Press, Boca Raton, Florida, p. 968
Westley M. S., Baratta G. A., Baragiola R. A., 1998, J. Chem. Phys., 108, 3321
Wood B. E., Roux J. A., 1982, J. Opt. Soc. Am., 72, 720
Yamada H., Person W. B., 1964, J. Chem. Phys., 41, 2478
Zanchet A., Rodriguez-Lazcano Y., Galvez O., Herrero V. J., Escribano R., Mate B., 2013, ApJ, 777, 26

This paper has been typeset from a TEX/LATEX file prepared by the author.